Hindawi Publishing Corporation
Smart Materials Research
Volume 2014, Article ID 145087, 10 pages
http://dx.doi.org/10.1155/2014/145087

Research Article

Thermoelastic and Pyroelectric Couplings Effects on Dynamics and Active Control of Smart Piezolaminated Beam Modeled by Finite Element Method

M. Sanbi,[1] R. Saadani,[2] K. Sbai,[2] and M. Rahmoune[2]

[1] *Team Science and Advanced Technologies, National School of Applied Sciences, Abdelmalek Essaadi University, 93030 Tetouan, Morocco*
[2] *Team Advanced Materials and Energy Systems, High School of Technology, Moulay Ismail University, 50040 Meknes, Morocco*

Correspondence should be addressed to M. Rahmoune; rahmoune@umi.ac.ma

Received 19 July 2014; Revised 13 October 2014; Accepted 27 October 2014; Published 24 November 2014

Academic Editor: Marcelo A. Trindade

Smart structures with integrated sensors, actuators, and control electronics are of importance to the next generation high-performance structural systems. In this study, thermopiezoelastic characteristics of piezoelectric beam continua are studied and applications of the theory to active structures in sensing and optimal control are discussed. Using linear thermopiezoelastic theory and *Timoshenko* assumptions, a generic thermopiezoelastic theory for piezolaminated composite beam is derived. Finite element equations for the thermopiezoelastic media are obtained by using the linear constitutive equations in Hamilton's principle together with the finite element approximations. The structure consists of a modeling of cantilevered piezolaminated *Timoshenko* beam with integrated thermopiezoelectric elements between two aluminium layers. The structure is modelled analytically and then numerically and the results of simulations are presented in order to visualize the states of their dynamics and the state of control. The optimal control *LQG* accompanied by the *Kalman filter* is applied. The effects of thermoelastic and pyroelectric couplings on the dynamics of the structure and on the control procedure are studied and discussed. We show that the control procedure cannot be perturbed by applying a thermal gradient and the control can be applied at any time during the period of vibration of the beam.

1. Introduction

In the development of distributed sensors, actuators, and thin-film devices, thin layer piezoelectrics (either laminated, deposited, or embedded) are of importance in many applications, for example, dynamic measurement, control, actuation, and so forth. In case studies of electromechanical coupling and implementation of the finite element method, several studies have been the subject of research on the topic covered in this paper. Aldraihem and Khdeir [1] have studied smart beams with extension and thickness-shear piezoelectric actuators. Trindade et al. [2] have investigated the piezoelectric active vibration control of damped sandwich beams. Gabbert et al. [3] have implemented the modeling, control, and simulation of piezoelectric smart structures using finite element method and optimal LQ control. Raja et al. [4] have analysed the active vibration control of composite sandwich beams with piezoelectric extension-bending and shear actuators. Moita et al. [5] have studied the active control of adaptative laminated structures with bonded piezoelectric sensors and actuators. Manjunath and Bandyopadhyay have used the technique of fast output sampling feedback in the control of vibrations in SISO based *Timoshenko* structures [6, 7]. Trindade and Benjeddou [8] have evaluated and optimized the effective electromechanical coupling coefficients of piezoelectric adaptive structures.

Besides mechanical and electric couplings and interactions, temperature can also influence the performance of piezoelectric devices and its variation can introduce voltage/charge generation in piezoelectric sensors. In addition, control voltage can cause temperature rise in piezoelectric actuators. Temperature can introduce the pyroelectric effect and the thermal strain effect to the distributed sensors and also thermal deflection in dynamic oscillations. Aouadi [9]

Table 1: Properties of the aluminium and piezoelectric layers.

Properties	Labels	Units	Beam *aluminium*	Sensor *PVDF biaxially oriented*	Actuator *PZT-5H32*	Foam
Length	$L_{b,s,a}$	(m)	0.2	0.04	0.04	0.04
Width	$l_{b,s,a}$	(m)	0.03	0.03	0.03	0.03
Thickness	$t_{b,s,a}$	(m)	0.001	0.001	0.001	0.001
Density	ρ	(g/cm^3)	8.03	1.78	7.7	0.7689
Young modulus	E	(GPa)	68	5.04	62	0.69
Piezoelectric stress constant	g_{31}	(Vm/N)	—	0.15	−9.11	—
Piezoelectric strain constant	d_{31}	$\times 10^{-12}$ (m/V)	—	4.34	−274	—
Pyroelectric constant	p	$\times 10^{-5}$ Cm^{-2} K^{-1}	—	−1.25	—	—
Dielectric constant	$\epsilon_{33}^S/\epsilon_0$	($\epsilon_0 = 8.85410^{-12}$ F/m)	—	12	3300	—
Damping	α	$\times 10^{-3}$	1	—	—	—
Constants	β	$\times 10^{-3}$	0.1	—	—	—
Thermal conductivity	K_d	(W/m·K)	—	1.5	1.5	—
Thermal expansion	α	$\times 10^{-6}$ (m/m·K)	—	140	3	—
Specific heat	c_0	J·kg^{-1}·K^{-1}	—	350	1.5	—

has discussed the generalized thermopiezoelectric problems with temperature-dependent properties. Ganesan and Sethuraman [10] have studied the thermally induced vibrations of piezothermoviscoelastic composite beam with relaxation times and system response. Sadek and Abukhaled [11] have implemented the optimal control of thermoelastic beam vibrations by piezoelectric actuation.

In this study, distributed sensing and control of a piezolaminated composite beam under sudden and intense thermal gradient have been studied and sensing/control demonstrated. The present work investigates the influence of the thermal and pyroelectric coupling on the dynamic behavior of the flexible composite piezolaminated beam and on the control procedure by the application of a thermal gradient on the faces of the structure. For this purpose, we consider a piezolaminated *Timoshenko*'s beam with sandwiched thermopiezoelectric sensors and actuators placed at different positions. The structure is modelled by finite element method where the linear constitutive equations in Hamilton's principle together with the finite element approximations are used. We look first for the effects of changes in temperature and position sensor on quality control by varying the sensor position along the beam. We are secondly looking if there is a decrease in the control quality when it is applied after the start of vibration of the beam. We demonstrate that the active control of the beam is influenced by the variation of temperature.

2. Basic Equations and FE Method Implementation

In this study, we consider a structure consisting of a cantilever composite piezolaminated beam ($L \times l \times t = 0.2 \times 0.03 \times 0.001$) with shear thermopiezoelectric layers (actuator or sensor) and a rigid foam both placed at the core of the structure and sandwiched between two relatively thick aluminum

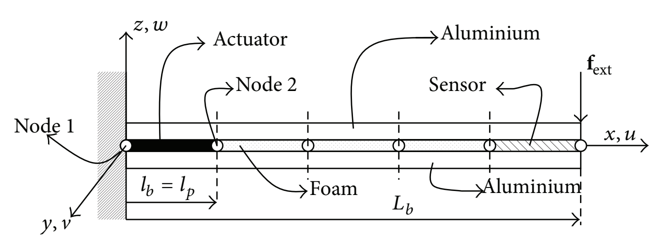

Figure 1: Cantilever beam with embedded thermopiezoelectric elements and the different models.

layers (Figure 1). The foam is introduced to fill the space between aluminium layers in order to obtain a compact beam. To obtain a better coupling between the main structure and piezoelectric layers, the center layers (thermopiezoelectric + foam) are considered perfectly bonded. Thickness, mass, and stiffness of the adhesive are considered relatively negligible. The beam is devised in 5 two-node finite beam elements (FE) where the actuator is fixed at the FE1 while the sensor occupies successively the four other finite elements (Figure 1). The physical, piezoelectric, pyroelectric, and thermal characteristics of the used beam and thermopiezoelectric elements (sensor and actuator) are given in the Table 1.

We start by giving equations of displacement, strain, and stress; then we give the constitutive equations and Hamilton's principle to the structure. In this work the following linear constitutive relations for thermopiezoelectric materials are employed [12]:

$$\begin{aligned} \{\sigma\} &= \left[C^E\right]\{\varepsilon\} - [e]\{E\} - [\lambda]\{\Theta\}, \\ \{D\} &= \left[e^T\right]\{\varepsilon\} - [\epsilon]\{E\} + [p]\{\Theta\}, \\ \{s\} &= [\lambda]^T\{\varepsilon\} + p^T\{E\} + [\tilde{\alpha}]\{\Theta\}, \end{aligned} \tag{1}$$

where the superscript S means that the values are measured at constant strain and the superscript E means that the values are measured at constant electric field, $\{\sigma\}$ is the stress tensor, $\{D\}$ is the electric displacement vector, $\{\Theta\}$ is temperature, $\{s\}$ is the entropy, and $\{E\}$ is the electric field. $\{\varepsilon\}$ is the strain tensor, $[C^E]$ is the elastic constants at constant electric field, $[e]$ denotes the piezoelectric stress coefficients, $[\epsilon]$ is the dielectric tensor at constant mechanical strain, $[\lambda]$ is the thermoelastic tensor, $[p]$ is the pyroelectric tensor, and $\tilde{\alpha}$ is the expansion coefficient with $\tilde{\alpha} = \rho_p c_0/\Theta_0$ where c_0 and Θ_0 are the specific heat and initial temperature, respectively.

Hamilton's principle is employed here to derive the finite element equations:

$$\int_{t_1}^{t_2} \left[\delta\left(T - U + W_e - W_{\text{th}}\right) + \delta W\right] dt = 0, \tag{2}$$

where t_1 and t_2 are two arbitrary instants, T is the kinetic energy, U is the potential energy, W_e denotes the work done by electrical forces, and W_{th} is the work done by thermal forces. The total kinetic energy T and the potential energy U of the composite beam are described by the following relations:

$$\begin{aligned}\delta T &= \left(I_1 \dot{u} + I_2 \dot{\theta}\right) \partial \dot{u} + I_1 \dot{w} \partial \dot{w} + \left(I_2 \dot{u} + I_3 \dot{\theta}\right) \partial \dot{\theta}, \\ \delta U &= N_x \left(\frac{\partial \delta U}{\partial x}\right) + M_x \left(\frac{\partial \delta \theta}{\partial x}\right) + Q_{xz} \left(\theta + \frac{\partial \delta w}{\partial x}\right).\end{aligned} \tag{3}$$

The work done by electrical forces and thermal forces and the element virtual works done by appliqued surface forces $\{f_A\}$ are given by

$$\begin{aligned}\delta W_e &= \{E\}^T \{D\} + \{p\} \{\Theta\}, \\ \delta W_{\text{th}} &= \{\varepsilon\}^T \{\lambda\} \{\Theta\}, \\ \delta W &= \{\delta q\}^T \{f_A\} - \delta \Phi \sigma_q.\end{aligned} \tag{4}$$

The mass moments characteristics of the cross-section of the beam are defined as

$$\left(I_1, I_2, I_3\right) = c \int_{-h_1}^{h_2} \rho_b \left(1, z, z^2\right) dz, \tag{5}$$

with ρ_b and $h_{1,2,3}$ being the mass density and the height of the beam + piezoelectric patches (the thickness of the total structure), respectively.

The dynamic equation can be found in [13], and the displacements $u(x)$ and $w(x)$ are written as

$$u(x,z) = u_0(x) + z\theta(x,t), \qquad w(x,z) = w_0(x), \tag{6}$$

where u_0, $w_0(x)$, and $\theta(x)$ are the axial, transverse midplane displacements and y-rotation, respectively [14]. Assuming that there is no compressibility in the z direction, the normal and transverse components of strain are:

$$\begin{aligned}\varepsilon_x &= \frac{\partial u_0}{\partial x} + z \frac{\partial \theta}{\partial x}, \qquad \varepsilon_z = 0, \\ \gamma_{xz} &= \frac{\partial u}{\partial x} + \frac{\partial w_0}{\partial x} = \left(\theta(x) + \frac{\partial w_0}{\partial x}\right).\end{aligned} \tag{7}$$

The beam constitutive equations can be written as

$$\begin{aligned}\begin{bmatrix} N_x \\ M_x \\ Q_{xz} \end{bmatrix} &= \begin{bmatrix} A_{11} & B_{11} & 0 \\ B_{11} & D_{11} & 0 \\ 0 & 0 & A_{55} \end{bmatrix} \left[\frac{\partial u_0}{\partial x} \quad \frac{\partial \theta}{\partial x} \quad \left(\theta + \frac{\partial w_0}{\partial x}\right) \right]^T \\ &\quad - \left[E_{11} \quad F_{11} \quad G_{55}\right]^T,\end{aligned} \tag{8}$$

where

$$\begin{aligned}N_x &= \int_{-h/2}^{h/2} c\sigma_x dz, \qquad M_x = \int_{-h/2}^{h/2} c\sigma_x z dz, \\ -Q_{xz} &= \int_{-h/2}^{h/2} c\tau_{xz} dz,\end{aligned} \tag{9}$$

where $\sigma_x = \overline{Q}_{11}$ is the extension stress, $\tau_{xz} = \overline{Q}_{55}$, γ_{xz} is the shear stress, c is the beam width, z is the distance measured between the plane of the structure and that of the kth layer laminate, h is the total thickness of the structure (beam + actuator/sensor + beam), N_x is the axial force, M_x is the bending moment, Q_{xz} is the shear force, $A_{11}, B_{11}, D_{11}, A_{55}$ are the extension, extension-bending, bending, and transverse shear stiffness coefficients given by [13, 15]

$$\begin{aligned}A_{11} &= c \sum_{k=1}^{n} \left(\overline{Q}_{11}\right)_k \left(z_k - z_{k-1}\right), \\ B_{11} &= \frac{c}{2} \sum_{k=1}^{n} \left(\overline{Q}_{11}\right)_k \left(z_k^2 - z_{k-1}^2\right), \\ D_{11} &= \frac{c}{3} \sum_{k=1}^{n} \left(\overline{Q}_{11}\right)_k \left(z_k^3 - z_{k-1}^3\right), \\ A_{55} &= c\mathbf{K} \sum_{k=1}^{n} \left(\overline{Q}_{55}\right)_k \left(z_k - z_{k-1}\right),\end{aligned} \tag{10}$$

where z_k is the distance of the kth layer relative to the x-axis, n is the number of layers, $\mathbf{K}$ is the correction shear deformation factor generally taken to be 5/6, and $\overline{Q}_{11}$, $\overline{Q}_{55}$ are calculated based on the physical properties of piezoelectric material [13, 15, 16]:

$$\begin{aligned}\overline{Q}_{11} &= Q_{11}\cos^4\lambda + Q_{22}\sin^4\lambda + 2\left(Q_{12} + Q_{66}\right)\sin^2\lambda\cos^2\lambda, \\ \overline{Q}_{55} &= G_{13}\cos^2\lambda + G_{23}\sin^2\lambda.\end{aligned} \tag{11}$$

The angle λ is the angle between the direction of the fibers and the longitudinal axis of the beam. The physical constants Q_{11}, Q_{22}, Q_{12}, Q_{66}, Q_{13}, Q_{23} relative to the foam, aluminum, and the piezoelectric material are

$$\begin{aligned}Q_{11} &= \frac{E_{11}}{1 - \nu_{12}\nu_{12}}, \qquad Q_{22} = \frac{E_{22}}{1 - \nu_{12}\nu_{12}}, \\ Q_{12} &= \frac{\nu_{12}E_{11}}{1 - \nu_{12}\nu_{12}}, \quad Q_{66} = G_{12}, \quad \frac{\nu_{12}}{E_{11}} = \frac{\nu_{12}}{E_{11}},\end{aligned} \tag{12}$$

where ν is the poisson coefficient and G is the rigidity transverse modulus. Respectively, E_{11}, F_{11}, and G_{55} are the induced piezoelectric axial force, bending moment due to deformation of the actuator, and the shear strength given by [13, 15]

$$E_{11} = c\sum_{k=1}^{n_a} \left(\overline{Q}_{11}\right)_k^a V^k(x,t)\, d_{31}^k,$$
$$F_{11} = \frac{c}{2}\sum_{k=1}^{n_a} \left(\overline{Q}_{11}\right)_k^a V^k(x,t)\, d_{31}^k \left(z_{k+}^a - z_{k-}^a\right), \quad (13)$$
$$G_{55} = c\mathbb{K}\sum_{k=1}^{n_a} \left(\overline{Q}_{55}\right)_k^a V^k(x,t)\, d_{15}^k.$$

Here, $E_{11} = F_{11} = 0$ since the piezoelectric layers are polarized longitudinally. $V^k(x,t)$ = the voltage applied to the kth actuator with thickness $(z_{k+}^a - z_{k-}^a)$ and piezoelectric constants d_{31}^k and d_{15}^k. N_a = the number of actuators. Consider

$$\{[u], [w], [\theta]\} = \{[N_u], [N_w], [N_\theta]\}\{\mathbf{q}\}, \quad (14)$$

where $q = [u_1 \;\; w_1 \;\; \theta_1 \;\; u_2 \;\; w_2 \;\; \theta_2]^T$ is the vector of nodal displacements and $[N_u]$, $[N_w]$, $[N_\theta]$ are the mode shape functions due to the axial displacement, transverse displacement, and the slop, which are defined as [17]

$$[N_u] = [N_1 \;\; N_2 \;\; N_3 \;\; N_4 \;\; N_5 \;\; N_6],$$
$$[N_w] = [N_7 \;\; N_8 \;\; N_9 \;\; N_{10}], \quad (15)$$
$$[N_\theta] = [N_{11} \;\; N_{12} \;\; N_{13} \;\; N_{14}].$$

The elements of the shape functions are given in [17]. The inertial forces vector $\mathbb{N}$ can be written as

$$\mathbb{N} = \begin{bmatrix} N_1 & N_2 & N_3 & N_4 & N_5 & N_6 \\ 0 & N_7 & N_8 & 0 & N_9 & N_{10} \\ 0 & N_{11} & N_{12} & 0 & N_{13} & N_{14} \end{bmatrix}\{q\}. \quad (16)$$

The mass matrix of the regular beam element is given by

$$\left[M^b\right] = \int_0^{l_b} [\mathbb{N}]^T [\mathbf{I}] [\mathbb{N}]\, dx, \quad (17)$$

where

$$I = \begin{bmatrix} I_1 & 0 & I_2 \\ 0 & I_1 & 0 \\ I_2 & 0 & I_3 \end{bmatrix} \quad (18)$$

is the inertia matrix. Similarly, the stiffness matrix of the regular beam element can be written as

$$\left[K^b\right] = \int_0^{l_b} [\mathbf{B}]^T [\mathbf{D}] [\mathbf{B}]\, A_b dx, \quad (19)$$

where A_b is the area of cross-section of the beam element and

$$\mathbf{B} = \frac{d\mathbb{N}}{dx}, \qquad \mathbf{D} = \begin{bmatrix} A_{11} & B_{11} & 0 \\ B_{11} & B_{11} & 0 \\ 0 & 0 & A_{55} \end{bmatrix}. \quad (20)$$

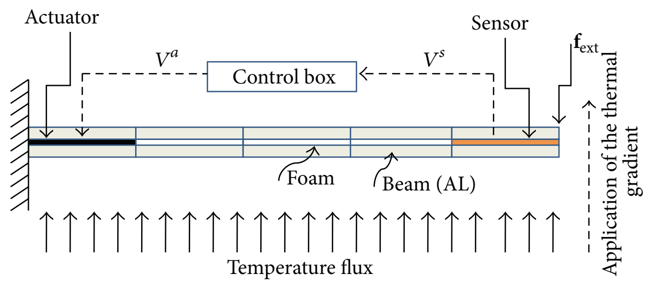

Figure 2: Application of a thermal gradient.

The mass and stiffness element matrices of the piezoelectric element are obtained in the same manner with respect to the physical characteristics of the material. The mass and stiffness of the finite elements which together contain the element of the beam and the piezoelectric element are given by $M = M^p + 2M^b$ and $K = K^p + 2K^b$.

The sensor output voltage, due to thermal and mechanical deformations and temperature (pyroelectric effect), can be written as

$$V^s(t) = \mathbf{S}^T\dot{\mathbf{q}} + p\dot{\Theta}, \quad (21)$$

where

$$\mathbf{S}^T = \frac{6c\eta}{-12\eta + l_b^2} G_c \{e_{15}[0 \;\; 2 \;\; -l_p \;\; 0 \;\; -2 \;\; l_p]\}, \quad (22)$$

and l_b is the beam element length which is equal to piezoelectric element length l_p, G_c is the controller gain, p is the pyroelectric constant, and η is a constant given by

$$\eta = \frac{D_{11}}{A_{55}}\left(\frac{\gamma B_{11}}{D_{11}} - 1\right), \qquad \gamma = \frac{B_{11}}{A_{11}}; \quad (23)$$

the control force developed by the thermopiezoelectric actuator is written

$$\mathbf{f}_{\text{ctrl}} = \mathbb{G} d_{15}\overline{h}\int_0^{l_p} N_\theta dx V^a(t) = \mathbf{h}V^a(t), \quad (24)$$

where $\mathbb{G}$ is the transverse module, $\overline{h} = (h_a + h_b)/2$ is the distance between neutral axes of the beam and the thermopiezoelectric layer, N_θ is the shape function of rotations, and $V^a(t)$ is the actuator input voltage.

Similarly, the forces due to thermoelastic and pyroelectric couplings $\mathbf{f}_{\text{eth}}$ and $\mathbf{f}_{\text{pth}}$ are given by

$$\mathbf{f}_{\text{eth}} = \int N_\Theta^T [\lambda] N_\Theta \Theta dA, \qquad \mathbf{f}_{\text{pth}} = \int N_\Theta^T [\mathbf{p}] N_\Theta \Theta dA, \quad (25)$$

where N_Θ is thermal shape function, $[\lambda]$ is the thermoelastic tensor, and $[\mathbf{p}]$ is pyroelectric tensor. If an external force $\mathbf{f}_{\text{ext}}$ is applied, the total force acting on the beam is

$$\mathbf{f}^t = \mathbf{f}_{\text{ext}} + \mathbf{f}_{\text{ctrl}} + \mathbf{f}_{\text{eth}} + \mathbf{f}_{\text{pth}}. \quad (26)$$

Therefore, the equation of motion can be written as

$$\mathbf{M}^*\ddot{\mathbf{g}} + \mathbf{C}^*\dot{\mathbf{g}} + \mathbf{K}^*\mathbf{g} = \mathbf{f}_{\text{ext}}^* + \mathbf{f}_{\text{ctrl}}^* + \mathbf{f}_{\text{eth}}^* + \mathbf{f}_{\text{pth}}^*, \quad (27)$$

where $\mathbf{M}^*$, $\mathbf{K}^*$, $\mathbf{C}^*$, and $\mathbf{g}$ are the generalized mass, stiffness, damping matrices, and generalized displacement. The above

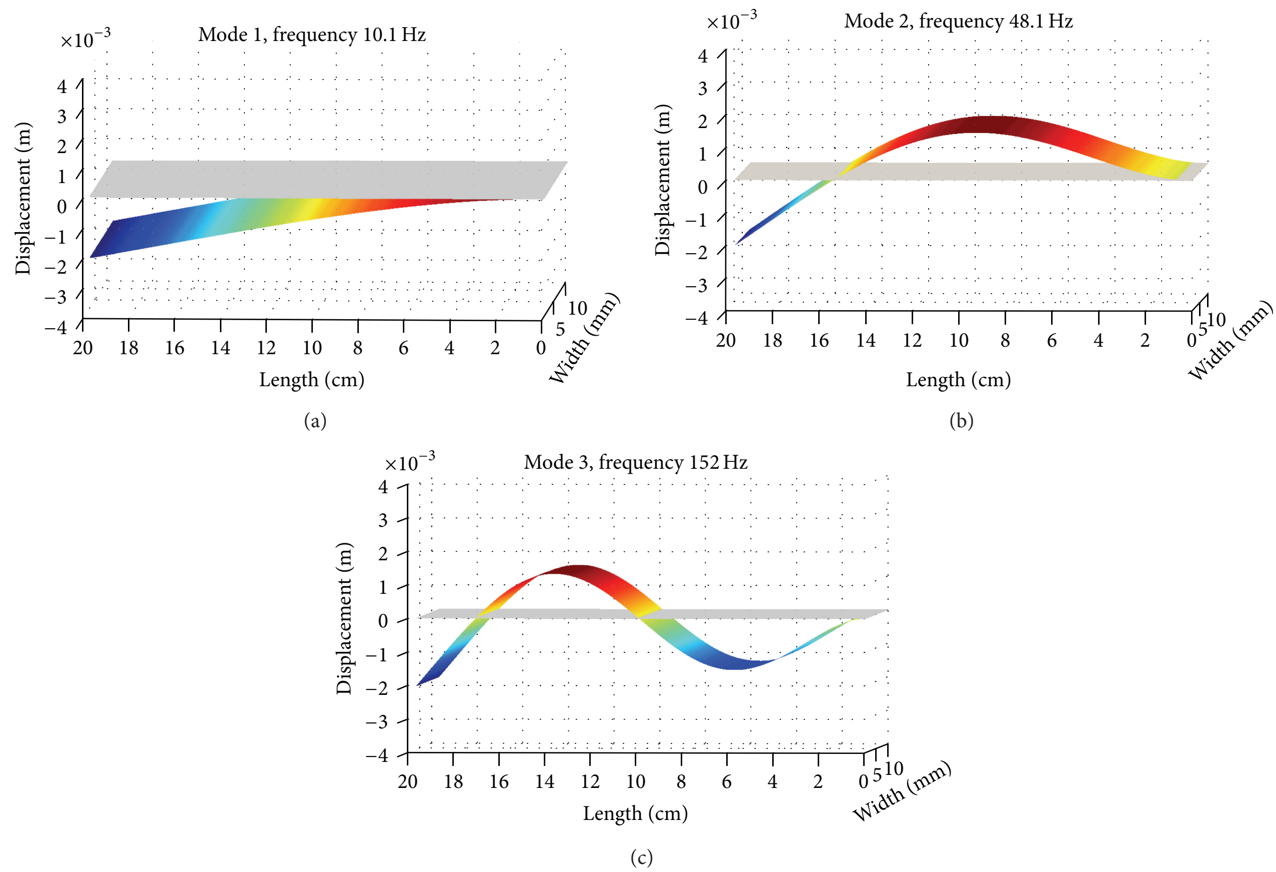

FIGURE 3: The first three modes of the beam subjected to a pulse of 2N at its free end.

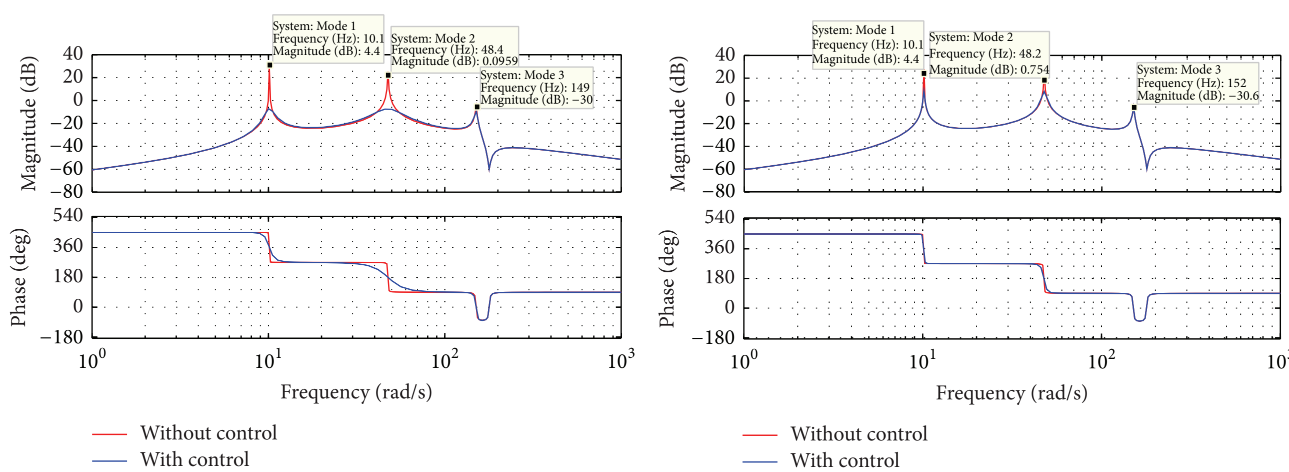

FIGURE 4: Spectra of the first three modes for the sensor positions EF5 and EF2 in *SISO* model, respectively.

equation can be transformed in state space model as

$$\dot{x} = \mathbf{A}x(t) + \mathbf{B}u(t) + \mathbf{E}r(t) + \mathbf{E}^{\text{th}},$$
$$y(t) = \mathbf{C}^{T}x(t) + \mathbf{D}u(t), \tag{28}$$

with

$$A = \begin{bmatrix} 0 & I \\ -\mathbf{M}^{*-1}\mathbf{K}^{*} & -\mathbf{M}^{*-1}\mathbf{C}^{*} \end{bmatrix},$$

$$B = \begin{bmatrix} 0 \\ \mathbf{M}^{*-1}\mathbf{T}^{T}\mathbf{h} \end{bmatrix},$$

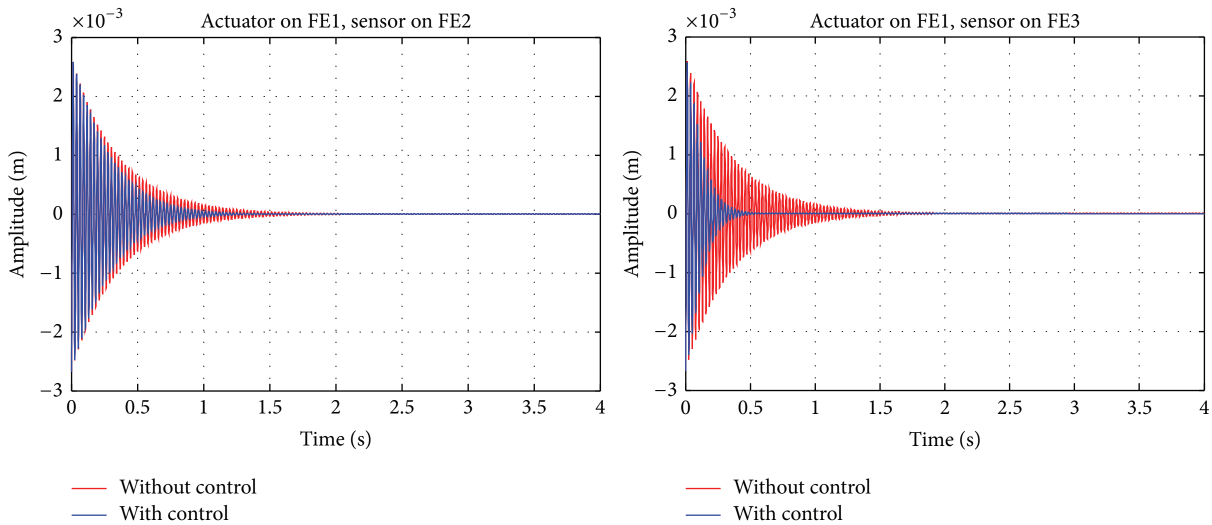

Figure 5: Influence of the sensor location on the quality of control in the case of a pulse excitation ($Q = 10^7$, $R = 1$, and controller gain $G_c = 200$) for the two first modes.

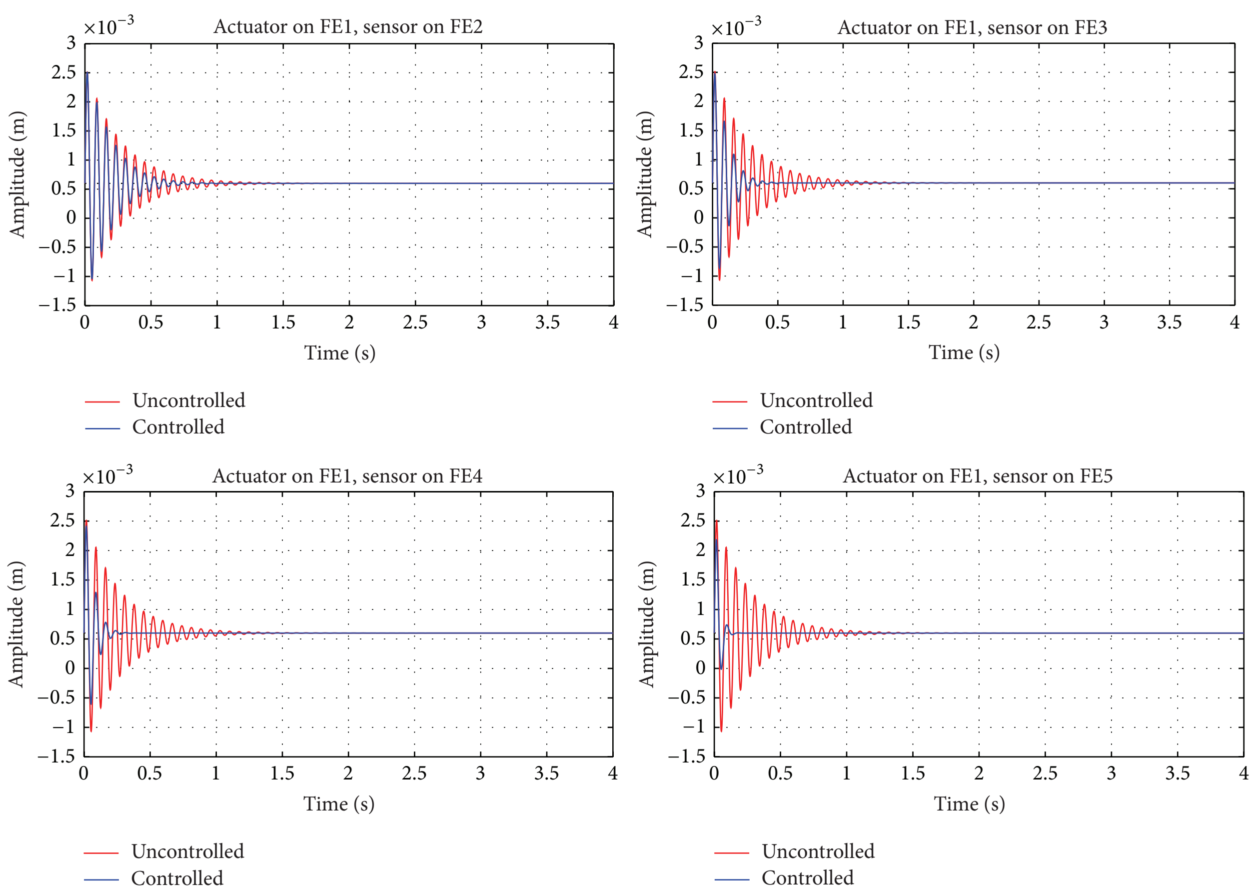

Figure 6: Influence of the sensor location on the quality of control in the case of a step excitation ($Q = 10^5$, $R = 1$, and controller gain $G_c = 200$) for the first mode.

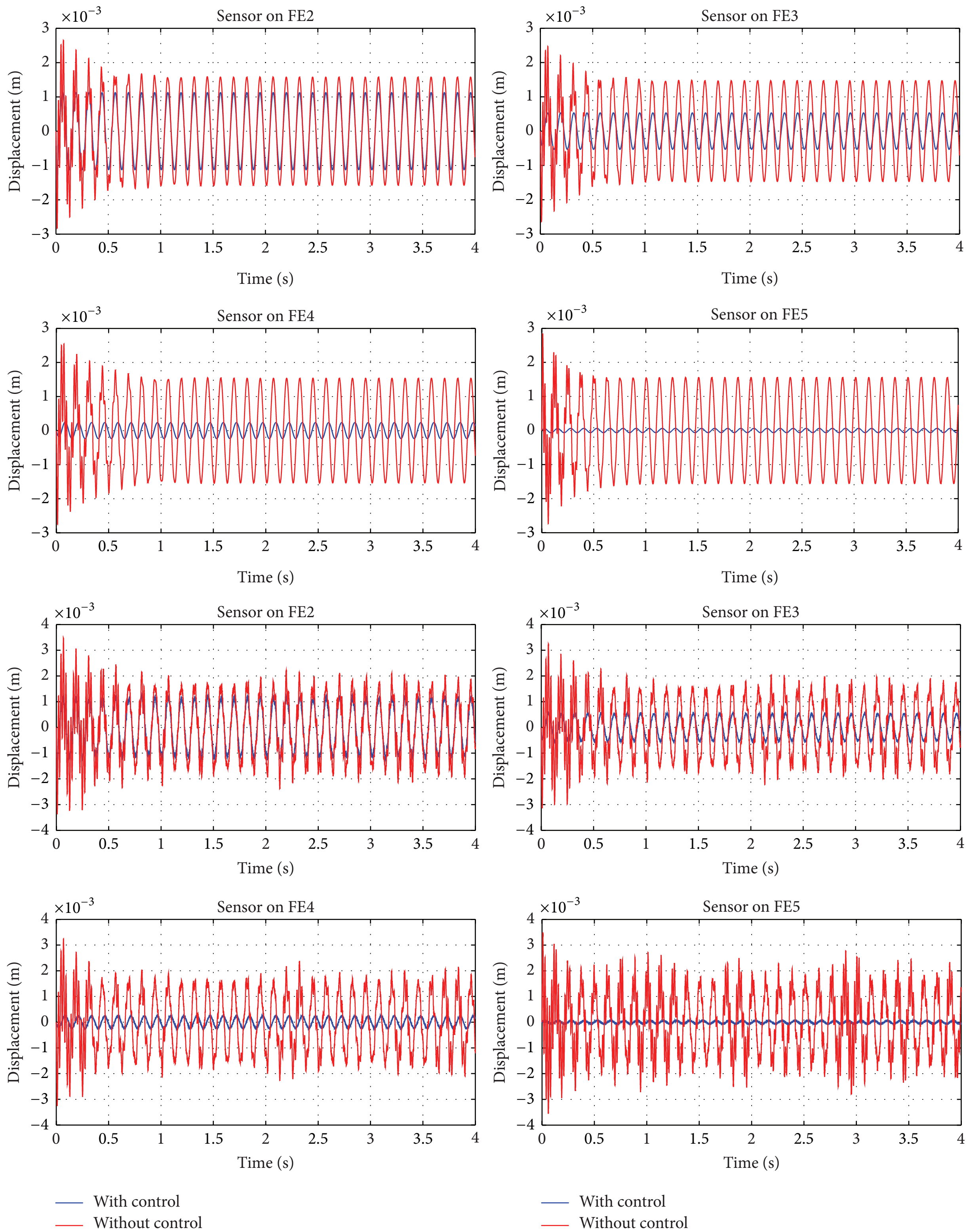

FIGURE 7: Displacement (without and with noise) of the beam subjected to a sinusoidal excitation $1.5\sin(50t)$ to its free end for ($Q = 10^{10}$, $R = 0.01$, and controller gain $G_c = 500$).

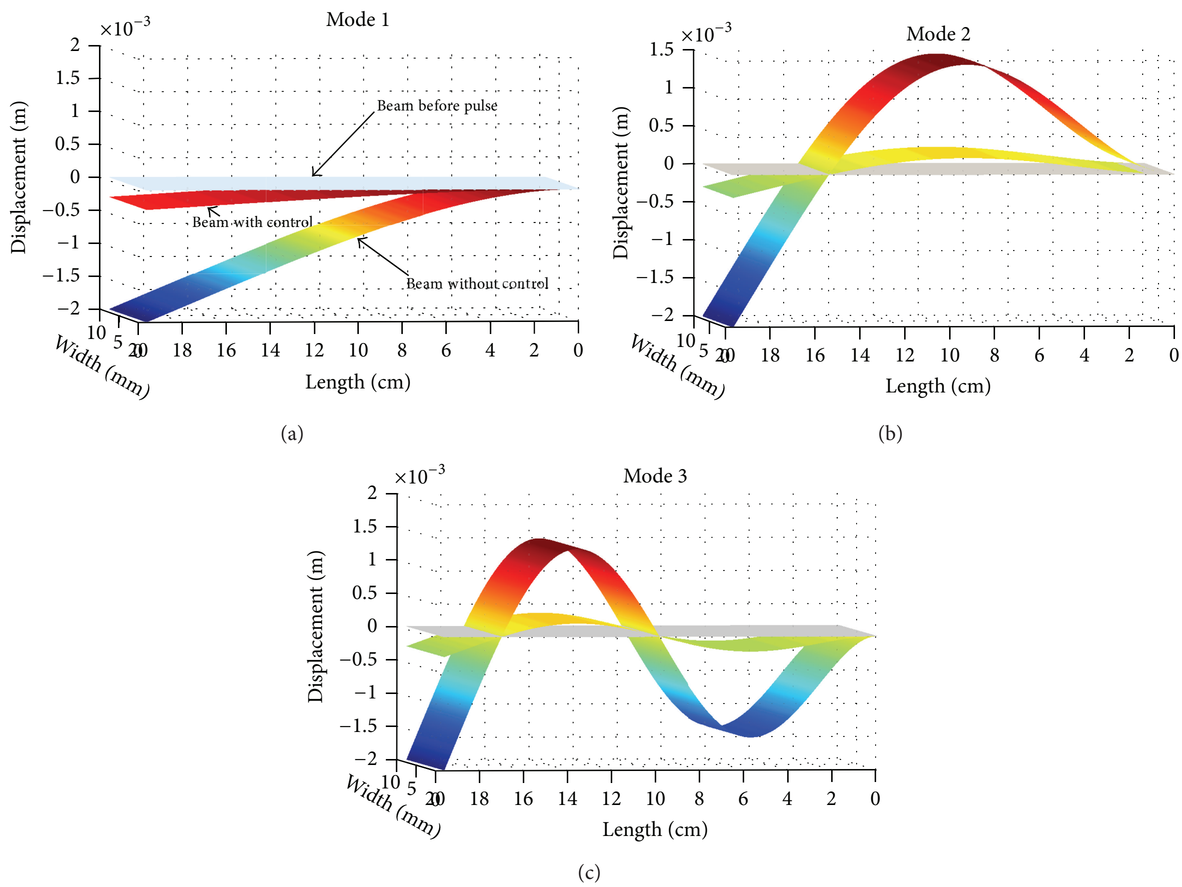

FIGURE 8: 3D control visualisation for the three first modes and for (2N) pulse excitation at free end of the beam, $Q = 10^6$, $R = 0.01$, and $G_c = 500$).

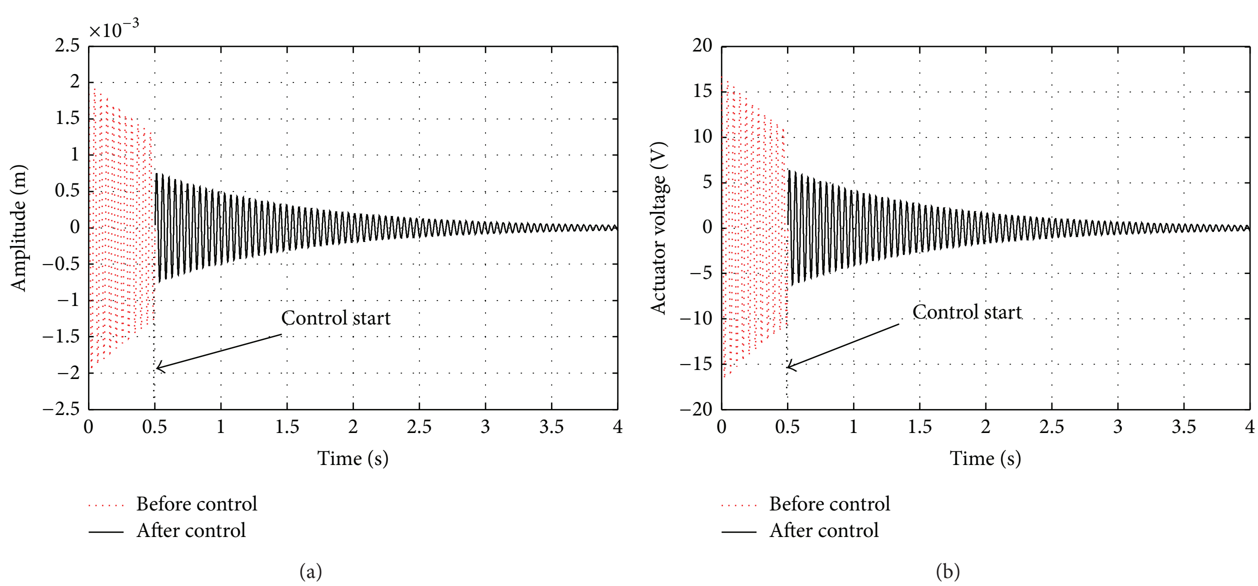

FIGURE 9: Application of control during the vibration of the beam.

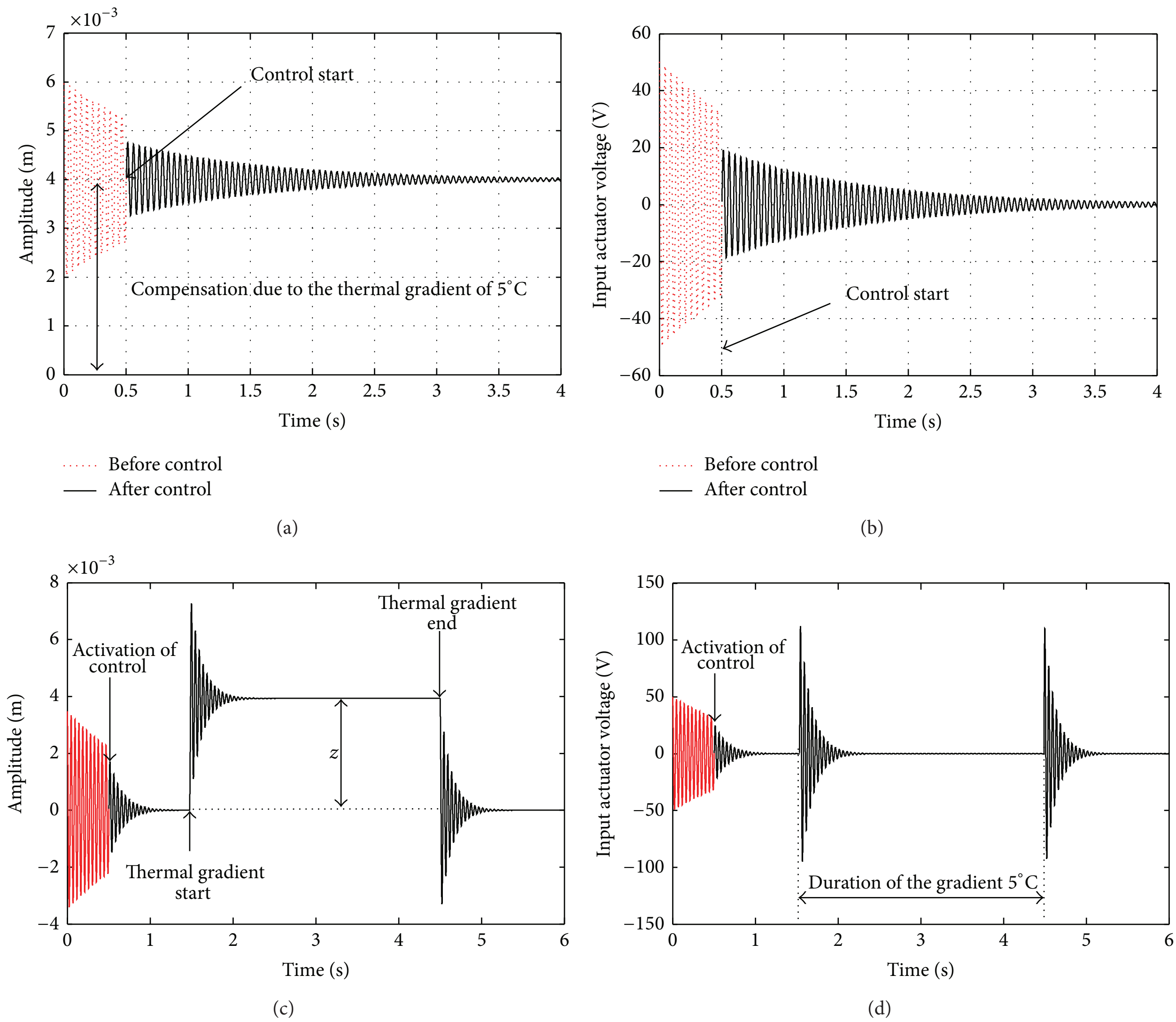

Figure 10: The responses of the dynamics of the beam before, during, and after the application of control and thermal gradient.

$$\mathbf{C} = \left[0 \ \ \mathbf{S}^T\mathbf{T}\right],$$

$$\mathbf{E} = \begin{bmatrix} 0 \\ \mathbf{M}^{*-1}\mathbf{T}^T \end{bmatrix} r(t),$$

$$\mathbf{E}^{\text{th}} = \begin{bmatrix} 0 \\ \mathbf{M}^{*-1}\mathbf{T}^T\left\{\mathbf{f}_{\text{eth}} + \mathbf{f}_{\text{pth}}\right\} \end{bmatrix}, \tag{29}$$

where $\mathbf{T}$ is the modal matrix, $u(t)$ is the command vector, and $r(t)$ is the external force vector.

3. Results and Discussion

The graphs presented below correspond to the responses of the free end of the beam. We compare noncontrolled and controlled responses for a disturbance in impulse (2N) before, during, and after applying a thermal gradient so that the faces of the structure are under two different temperatures as illustrated in Figure 2. We assume that the material with which the material bonded the thermopiezoelectric elements is resistant to the temperature change (the patches remain perfectly bonded to the surfaces of the beam). A thermal gradient will be applied to visualize the thermal and pyroelectric effect on the vibration behavior of the structure under thermal perturbations.

Figures 3 and 4 show the three first modes. The different responses, step, impulse, and sinusoidal are illustrated in the Figures 5, 6, and 7. Figure 8 shows 3D control visualisation for the three first modes and for (2N) pulse excitation at free end of the beam.

Figure 10 shows in 3D the deflection of the beam under a 5°C thermal gradient. In addition to the sensor voltage created by the expansion of the beam under the thermal field, another voltage is created by the temperature increase (pyroelectric effect). In fact, respectively, Figures 9 and 10 show the variation of amplitude and voltage at the input of the actuator for the beam before and during the control applied

0.5 sec after the application of the pulse. The control method can be applied during the vibration without diminishing its quality or effectiveness. The same above figures illustrate the thermal compensation of responses in amplitude and voltage of the actuator. The gradient is applied at the beginning of the pulse after 0.5 sec. We noticed that the application of such a gradient did not alter the quality and effectiveness of control. The effectiveness of control will depend on the intensity of the thermal gradient and its duration. Indeed, the intense gradients can infect the pyroelectric effect in the thermopiezoelectric elements and deteriorate their polarization. We finally conclude that the control method used is better adapted to sudden changes in disturbance types of vibration or for small variations in the thermal gradient. To show the influence of thermal effect on the used control method, we maintain a gradient for 3 sec. We note that the control procedure is effective in applying or removing the thermal gradient. However, the application of a constant gradient for a long duration can not be monitored or controlled by the method *LQG*. Instead, the sudden application of a gradient is controllable. This is one of the advantages of this method, since all the thermal disturbances are unpredictable. We conclude, therefore, that the control method used is effective for sudden changes in temperature.

4. Conclusion

Modeling by the finite element method according to the theory of *Timoshenko*, of a cantilever piezolaminated composite beam with embedded thermopiezoelectric element, is presented. The optimal control based on the method of *LQG-Kalman* is applied and discussed. The influence of the location of the sensor and of the application of thermal gradient on the effectiveness of control is analyzed. In fact, our analysis shows that the more the sensor is near the free end of the beam, the more the control is effective. This is due to the the increase of the deformation amplitudes in the sensor, which affects the control voltage of the actuator. We have also shown that the application of control during the vibration of the structure does not diminish the control quality; that is, the control can be applied at any time during the vibration of the beam. Moreover, the deformations produced by the sudden application of a thermal gradient can be controlled. We reported that the application of an intense thermal gradient, or of long duration, can infect the pyroelectric effect in the sensor or may deteriorate the polarization of the actuator.

Conflict of Interests

The authors declare that there is no conflict of interests regarding the publication of this paper.

References

[1] O. J. Aldraihem and A. A. Khdeir, "Smart beams with extension and thickness-shear piezoelectric actuators," *Smart Materials and Structures*, vol. 9, no. 1, pp. 1–9, 2000.

[2] M. A. Trindade, A. Benjeddou, and R. Ohayon, "Piezoelectric active vibration control of damped sandwich beams," *Journal of Sound and Vibration*, vol. 246, no. 4, pp. 653–677, 2001.

[3] U. Gabbert, T. Trajkov-Nestorović, and H. Köppe, "Modelling, control and simulation of piezoelectric smart structures using finite element method and optimal LQ control," *Facta Universitatis Series: Mechanics, Automatic Control and Robotics*, vol. 3, no. 12, pp. 417–430, 2002.

[4] S. Raja, G. Prathap, and P. K. Sinha, "Active vibration control of composite sandwich beams with piezoelectric extension-bending and shear actuators," *Smart Materials and Structures*, vol. 11, no. 1, pp. 63–71, 2002.

[5] J. M. S. Moita, I. F. P. Correia, C. M. M. Soares, and C. A. M. Soares, "Active control of adaptive laminated structures with bonded piezoelectric sensors and actuators," *Computers & Structures*, vol. 82, no. 17–19, pp. 1349–1358, 2004.

[6] T. C. Manjunath and B. Bandyopadhyay, "Control of vibrations in flexible smart structures using fast output sampling feedback technique," *International Journal of Computational Intelligence*, vol. 3, no. 2, pp. 127–141, 2006.

[7] T. C. Manjunath and B. Bandyopadhyay, "Mathematical modeling of SISO based Timoshenko structures—a case study," *International Journal of Mathematics Sciences*, vol. 1, no. 1, pp. 1–19, 2007.

[8] M. A. Trindade and A. Benjeddou, "Effective electromechanical coupling coefficients of piezoelectric adaptive structures: critical evaluation and optimization," *Mechanics of Advanced Materials and Structures*, vol. 16, no. 3, pp. 210–223, 2009.

[9] M. Aouadi, "Generalized thermo-piezoelectric problems with temperature-dependent properties," *International Journal of Solids and Structures*, vol. 43, no. 21, pp. 6347–6358, 2006.

[10] N. Ganesan and R. Sethuraman, "Thermally induced vibrations of piezo-thermo-viscoelastic composite beam with relaxation times and system response," *Multidiscipline Modeling in Materials and Structures*, vol. 6, no. 1, pp. 120–140, 2010.

[11] I. Sadek and M. Abukhaled, "Optimal control of thermoelastic beam vibrations by piezoelectric actuation," *Journal of Control Theory and Applications*, vol. 11, no. 3, pp. 463–467, 2013.

[12] J. S. Yang and R. C. Batra, "Free vibrations of a linear thermopiezoelectric body," *Journal of Thermal Stresses*, vol. 18, no. 2, pp. 247–262, 1995.

[13] H. Abramovich, "Deflection control of laminated composite beams with piezoceramic layers—closed form solutions," *Composite Structures*, vol. 43, no. 3, pp. 217–231, 1998.

[14] G. Shi and K. Y. Lam, "Finite element vibration analysis of composite beams based on higher-order beam theory," *Journal of Sound and Vibration*, vol. 219, no. 4, pp. 707–721, 1999.

[15] L. Edery-Azulay and H. Abramovich, "Piezoelectric actuation and sensing mechanisms—closed form solutions," *Composite Structures*, vol. 64, no. 3-4, pp. 443–453, 2004.

[16] J. R. Vinson and R. L. Sierakowski, *The Behavior of Structures Composed of Composites Materials*, Martinus Nijhoff, The Hague, The Netherlands, 1986.

[17] J. R. Banerjee, "Free vibration of sandwich beams using the dynamic stiffness method," *Computers and Structures*, vol. 81, no. 18-19, pp. 1915–1922, 2003.